Discovery of a Potent and Selective Protein Kinase CK2 Inhibitor by High-Throughput Docking

Eric Vangrevelinghe,[†] Kaspar Zimmermann,[‡] Joseph Schoepfer,[†] Robert Portmann,[§] Doriano Fabbro,[†] and Pascal Furet*,[†]

Oncology Research, Novartis Pharma AG, 4002 Basle, Switzerland, and Nervous System Research, Novartis Pharma AG, CH-4002 Basle, Switzerland, and Process R&D, Novartis Pharma AG, CH-4002 Basle, Switzerland

Received February 28, 2003

To assess the potential of protein kinase CK2 as a target for developing new antitumor agents, we have undertaken a search for inhibitors of this enzyme. As part of this effort, we report here the discovery of the potent and selective CK2 inhibitor (5-oxo-5,6-dihydroindolo[1,2-*a*]-quinazolin-7-yl)acetic acid. We identified this inhibitor of a novel structural type by high-throughput docking of our corporate compound collection in the ATP binding site of a homology model of human CK2, using an appropriate protocol. The synthesis of the inhibitor as well as that of related analogues whose CK2 inhibitory activities give support to the binding mode proposed by the docking program is described. The results obtained suggest that virtual screening of a 3D database by molecular docking is a useful approach for lead finding provided that adapted postdocking filtering and reranking procedures are applied to the primary hit list.

Introduction

Protein kinase CK2 (casein kinase II) is a ubiquitous, constitutively active, protein kinase with the distinctive properties of possessing hundreds of known phosphorylation protein substrates and accepting both ATP and GTP as cofactor.[1] Although the precise functions of CK2 in eukaryotes are still under intense investigation, roles in cell growth, proliferation, and survival have been established consistent with the fact that many of its substrates are proteins involved in signal transduction, the regulation of the cell cycle, or apoptosis.[2,3] Of particular interest for anticancer agents research are reports suggesting a role of CK2 in neoplastic growth.[4,5] For instance, it has been reported that overexpression of the catalytic subunit of CK2 can cause lymphoma.[6]

To elucidate the different cellular functions of CK2 and assess its potential as a therapeutic target in oncology, potent and selective small molecule inhibitors of its enzymatic activity are required. To date, two main types of chemical inhibitors of CK2 have been described.[7] The first type consists of polyhydroxylated aromatic compounds that include natural product derivatives with anthraquinone, fluorenone, flavone, and xanthenone core structures. Halogenated benzimidazole and benzimitriazole compounds form the second type. All these compounds are ATP site-directed inhibitors, and for several of them the structural basis of inhibition has been revealed with full atomic details by the determination of a X-ray cocrystal structure with the catalytic unit of *Zea mays* CK2.[8−10] In particular, this is the case with the halogenated benzimitriazole compound TBB, a very selective CK2 inhibitor (Chart 1).[11] Interestingly, despite a rather modest CK2 inhibitory potency lying in the micromolar range, this compound has been shown to induce apoptosis in Jurkat cells.[12] Compounds with increased potency would therefore appear very promising in the study of the cellular effects of CK2 inhibition. More potent inhibitors such as DAA exist in the natural product class, but they are less selective.

Chart 1. Previously Reported CK2 Inhibitors: 4,5,6,7-Tetrabromo-1*H*-benzotriazole (TBB) and 1,4-Diamino-5,8-dihydroxyanthraquinone (DAA)

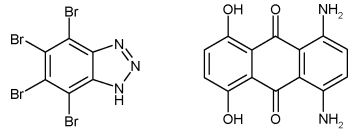

Considering CK2 as a possible target in our oncology programs, we wondered whether we could identify, in the Novartis collection of compounds, CK2 inhibitors having the same level of selectivity as TBB but showing higher potency. The availability of crystal structure information on the target prompted us to envisage a structure-based strategy for this purpose. Some recent reports of success in the discovery of biologically active molecules by high-throughput docking of large collections of compounds in a binding site of known structure[13,14] motivated us to try this approach in our quest for CK2 inhibitors. In this article, we describe this virtual screening experiment targeting the ATP binding site of CK2.

Results and Discussion

Homology Modeling. Virtual screening by docking requires an accurate three-dimensional (3D) structure of the considered target. While several crystal structures of the catalytic subunit of CK2 (CK2α) from *Zea mays* have been published in the past years and their coor-

* Corresponding author. Tel 41 61 696 79 90, fax 41 61 696 62 46, e-mail pascal.furet@pharma.novartis.com.
[†] Oncology Research, Novartis Pharma AG.
[‡] Nervous System Research, Novartis Pharma AG.
[§] Process R&D, Novartis Pharma AG.

10.1021/jm030827e CCC: $25.00
Published on Web 05/21/2003

```
Zea mays   34   YEVVRKVGRGKYSEVFEGINVNNNEKCIIKILKPVKKKKIKREIKILQNL
                 xx   x          x  xx    Xxx                 x
Human      39   YQLVRKLGRGKYSEVFEAINITNNEKVVVKILKPVKKKKIKREIKILENL

Zea mays   84   CGGPNIVKLLDIVRDQHSKTPSLIFEYVNNTDFKVLYPTLTDYDIRYYIY
                X     xX X   x XX x  x x  x       X  X        x x
Human      89   RGGPNIITLADIVKDPVSRTPALVFEHVNNTDFKQLYQTLTDYDIRFYMY

Zea mays  134   ELLKALDYCHSQGIMHRDVKPHNVMIDHELRKLRLIDWGLAEFYHPGKEY
                 x         x                 X                x
Human     139   EILKALDYCHSMGIMHRDVKPHNVMIDHEHRKLRLIDWGLAEFYHPGQEY

Zea mays  184   NVRVASRYFKGPELLVDLQDYDYSLDMWSLGCMFAGMIFRKEPFFYGHDN
                              X X             x x          x
Human     189   NVRVASRYFKGPELLVDYQMYDYSLDMWSLGCMLASMIFRKEPFFHGHDN

Zea mays  234   HDQLVKIAKVLGTDGLNVYLNKYRIELDPQLEALVGRHSRKPWLKFMNAD
                x    x       xX XX xx  X     xxxXxx      X Xx xxxx
Human     239   YDQLVRIAKVLGTEDLYDYIDKYNIELDPRFNDILGRHSRKRWERFVHSE

Zea mays  284   NQHLVSPEAIDFLDKLLRYDHQERLTALEAMTHPYF
                        x           X    X   X
Human     289   NQHLVSPEALDFLDKLLRYDHQSRLTAREAMEHPYF
```

Figure 1. Alignment of *Zea mays* and human CK2α sequences. Residues corresponding to the ATP binding site are marked in bold type. Uppercase X symbol indicates a totally different residue while lowercase x symbol indicates a similar residue.

dinates made public, those of the recently determined crystal structure of human CK2[15] were not publicly available at the time of this work. However, the high degree of conservation between the sequences of CK2α in *Homo sapiens* and *Zea mays* allowed us to construct an accurate 3D homology model of human CK2α, our target, based on one of the *Zea mays* structures. The amino acid identity between the human and the *Zea mays* sequences is equal to 72% and reaches 82% if only the 22 residues forming the ATP binding site are considered. The alignment reported in Figure 1 shows the strong similarity of the two sequences. Thus, we expected that a homology model of human CK2α based on this alignment would have a degree of accuracy that made it suitable for structure-based ligand design and molecular docking studies. We could confirm a posteriori the accuracy of our model by comparing it to the crystal structure of Niefind et al.[15] when it became available very recently. The root-mean-square deviation (rmsd) between the coordinates of the main chain Cα atoms of our CK2 homology model and those of the crystallographic structure calculated on the entire catalytic kinase domain has a value of 0.92 Å. Considering only the 22 residues forming the ATP binding site, this is only 0.64 Å. These rmsd values are significantly lower than the resolution of the crystallographic structure (3.1 Å), thus validating the use of our homology model for virtual screening purpose.

Virtual Screening Procedure. Our objective was to screen a large subset of our corporate collection of compounds containing around 400 000 structures. To achieve this goal within a reasonable time frame, we needed a fast and robust docking tool. The software DOCK, regarded as fulfilling these criteria, was selected for this task. DOCK, developed by Kuntz and coworkers, has shown promise as a tool for the identification of macromolecule ligands via database searching.[16] Some successful applications of DOCK in drug discovery research have already been claimed. These include the identification of inhibitors for the HIV-1 protease,[17] thymidylate synthase,[18] influenza hemagglutinin,[19] and parasitic proteases.[20]

DOCK requires that the binding site of the target be defined using spheres that complement the molecular surface of the receptor. The centers of these spheres can be thought of as pseudo-atom positions onto which DOCK superimposes atoms of the database molecules to generate a ligand orientation in the binding site. Only spheres that fill the ATP binding site and more precisely the region close to the hinge segment of CK2 have been considered in this experiment (Figure 2). In protein kinases, the hinge segment is the amino acid stretch that connects the N- and C-terminal domains at the interface of which the ATP binding site is located. The region close to the hinge segment is the most hydrophobic and solvent-shielded part of the ATP pocket and consequently inhibitors usually form their most productive interactions with amino acid residues of this region. This is why spheres located at the solvent exposed entrance of the cavity, toward which the triphosphate chain of ATP extends, were considered less important and discarded to speed up the calculations.

Although the docking protocol used (see details in the Experimental Section) has been developed internally on several case studies and has demonstrated its ability to rank known inhibitors for similar targets at the top of the hit list, we decided to apply in this case all the postprocessing filtering and reranking tasks that are recommended to increase the hit rate in large database docking.[21] Thus, we successively applied the three following postprocessing treatments to the primary hit list:

- The first stage was a filtering of the hit list based on pharmacophore information. Hydrogen bonding to the hinge segment is a key determinant of binding affinity to the ATP pocket of protein kinases as testified by the presence of this interaction in almost all the available X-ray crystal structures of inhibitor-kinase complexes.[22−24] Best scored candidates were thus examined in terms of the presence or absence of this interaction. Compounds not forming a hydrogen bond interaction with the hinge segment were removed.

- In a second stage, following a consensus scoring approach, we applied to the hit list the scoring function developed by Wang et al.[25] Only the compounds best scored by this function were retained.

- The last stage was the unavoidable visual inspection of the remaining top ranked candidates docked in the ATP binding site of CK2. This crucial step allowed us to discard compounds exhibiting unfavorable interactions with the binding site or adopting unrealistic conformations as a result of the shortcomings of the scoring functions.

Biological Results. Following the above procedure, a dozen of compounds were finally selected and ordered from the Novartis chemical archives for actual testing in a CK2 phosphorylation inhibition assay. In the assay, four of the selected compounds turned out to inhibit more than 50% of the enzymatic activity of CK2 at a concentration of 10 μM. The other eight compounds were only marginally active, inhibiting less than 50% of the activity of the enzyme at the same concentration. Among the four active compounds, which belong to different chemical classes, the most potent one, exhibiting 97% inhibition at a concentration of 10 μM, legitimately retained our attention. This compound, **4**, is an indoloquinazolinone derivative synthesized at Novartis in an unrelated medicinal chemistry project (Chart 2). Its IC_{50} value for CK2 inhibition was determined (Table 1). With

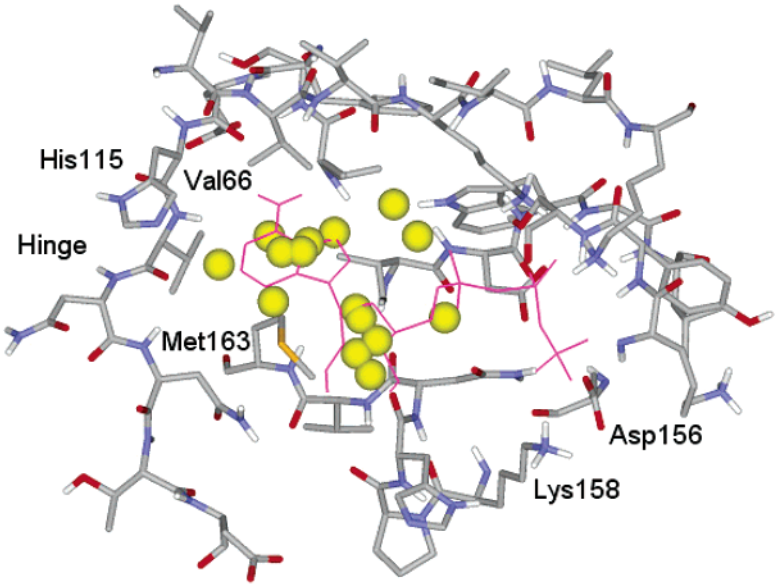

Figure 2. Overlay of the docking site points used (yellow spheres) and the ATP analogue extracted from the crystallographic template structure 1DAW (magenta) inside the active site of the homology model of human CK2α.

Chart 2.
(5-Oxo-5,6-dihydroindolo[1,2-*a*]quinazolin-7-yl)acetic Acid (4) Retrieved from the Novartis Compound Collection

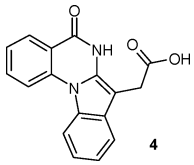

Table 1. CK2 Inhibitory Potency of Several 7-Substituted Indoloquinazolinone Derivatives

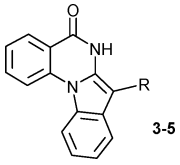

	R	IC_{50} (μM)[a]	% inhib at 10 μM
3a	CH_3	nd	*12*
4	CH_2COOH	0.080	*97*
5	CH_2CH_2OH	nd	48

[a] The data represent averages of at least three determinations.

a value of 80 nM, we had discovered the most potent inhibitor of the CK2 kinase ever reported. **4** showed in addition a remarkable specificity for CK2 when assayed for inhibition of 20 other kinases as reported in Table 2. None of the other kinases, representative of different subfamilies, was inhibited more than 50% by **4**.

The binding pose found by DOCK for this compound in the ATP pocket of our homology model of human CK2α is shown in Figure 3. As can be seen, the docking program positioned **4** in the pocket in such a way that its lactam moiety makes bidendate hydrogen bonds with the backbone of residue Val 116 of the hinge segment. This allows multiple hydrophobic interactions to be made between the polycyclic core of the molecule and residues Leu 45,Val 53, Val 66, Met 163, and Ile 174 that normally form the environment of the adenosine part of ATP in the enzyme pocket. Such interactions including the canonical hydrogen bonds to the hinge segment are characteristic of potent protein kinase inhibitors as revealed by numerous crystal structures, particularly that of the anthraquinone inhibitor DAA in complex with CK2, recently published.[10] Hence, we judged the binding mode proposed by DOCK for compound **4** as quite plausible.

Of particular interest in the binding model is the salt bridge formed by the 7-acetic acid group of **4** and residue Arg 43 located on the side of the pocket opened to solvent. This interaction drew our attention for two reasons. First, the model suggested that it plays a significant role in the potency of the compound because such ionic interactions are usually very strong. Second, we speculated that it may also play a role in the high selectivity displayed by **4** since Arg 43 is not conserved within the protein kinase family. For instance, in the c-Src and c-Abl kinases, which are very poorly inhibited by **4**, this position is occupied by a valine and a histidine residue, respectively.

To check the importance of the 7-acetic acid group, suggested by the model, we tested two available analogues of **4** lacking an acid function to form the putative salt bridge with Arg 43. Their chemical structures and CK2 inhibition potencies are summarized in Table 1. With an inhibitory activity of 12% at 10 μM, the analogue with a 7-methyl substituent, **3a**, is dramatically less potent than **4**. The 7-hydroxyethyl analogue **5**, having an inhibitory activity of 48% at 10 μM, is also less active than **4** but to a lesser extent. The binding model is consistent with these results. Completely abolishing any polar interaction with Arg 43, as in compound **3a**, is expected to be more detrimental to potency than replacing a salt bridge interaction by a weaker hydroxyl−guanidinium hydrogen bond as it is done going from **4** to **5**. Thus, support for the binding hypothesis was gained from this structure−activity relationship data.

Chemistry. 7-Substituted indoloquinazolinones are described only twice in the literature so far. Moore et al.[26] reported on the synthesis of the 7-phenyl derivative

Table 2. Selectivity Profile of Compound **4** in Terms of % of Inhibition of the Catalytic Activity of the Kinases at a Compound Concentration of 10 μM

CK2	c-Abl	HER-1	HER-2	KDR	Flt-3	IGF-1R	c-Raf-1	PDGFR-ß	c-Kit	Flt-4	Flt-1	Tek	PKA	c-src	CDK1	PKB	PDK1	Ins-R	FGFR-1	c-Met
97	25	12	29	54	41	44	30	11	31	30	21	36	51	0	51	30	9	23	32	40

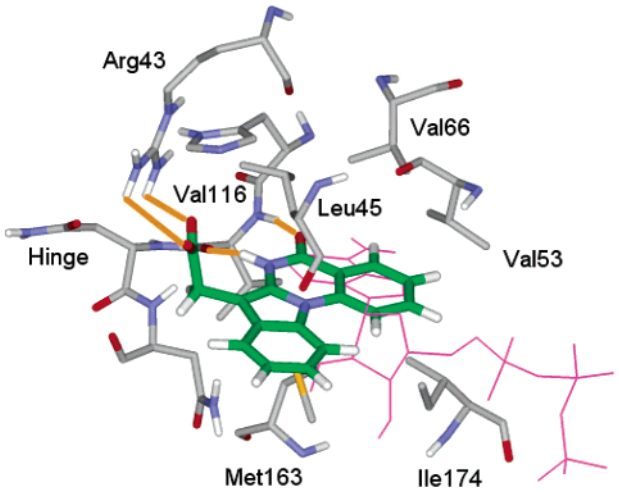

Figure 3. Relative binding modes of compound **4** (green) and the ATP analogue extracted from the crystallographic template structure 1DAW (magenta) in the human CK2α active site. The hydrogen bonds formed with Arg 43 and Val 116 are indicated as orange lines.

synthesized via cyclodehydration from α,α-diphenylquinazolinonemethanol. Moehrle and Seidel[27] described the formation of a hexacyclic indoloquinazolinone derivative obtained by condensation of anthranilic acid methyl ester and coumaranone. None of these methods is suited to produce derivatives with different substituents in position 7 of the indoloquinazolinone skeleton.

Our synthesis is based on the rearrangement of a substituted 11-oxo-10,11-dihydro-5*H*-dibenzo[*b*,*f*]azepine-10-carbonitrile into the indoloquinazolinone skeleton under basic conditions. No studies were undertaken to elucidate the mechanism. It is believed, however, that the rearrangement sequence starts by attack of the carbonyl group of the oxodibenzazepine by methoxide, leading to ring-opening. Subsequent intramolecular nucleophilic attack of the azepine nitrogen on the C-atom of the cyano group may push the cyano nitrogen to attack the ester carbonyl leading to the tetracyclic skeleton of the target molecules. Subsequent aromatization concludes the rearrangement. To our knowledge such a reaction is unprecedented.

Our synthesis (see Scheme 1) of the derivatives substituted in position 7 started by migrating the cyano group of 10-oxo-10,11-dihydrodibenzo[*b*,*f*]azepine-5-carbonitrile to position 11 under basic conditions giving **1**. Subsequently, carbon-11 can easily be alkylated, e.g., with methyl iodide to **2a** or ethyl bromoacetate to **2b**. The rearrangement described above occurs upon treatment with sodium methoxide in methanol yielding **3a** and **3b**, respectively. This two-step alkylation−rearrangement sequence can be done in one-pot and is suited for automated parallel synthesis, e.g., on a Quest synthesizer.[28] The carboxylic acid **4** was obtained by

Scheme 1

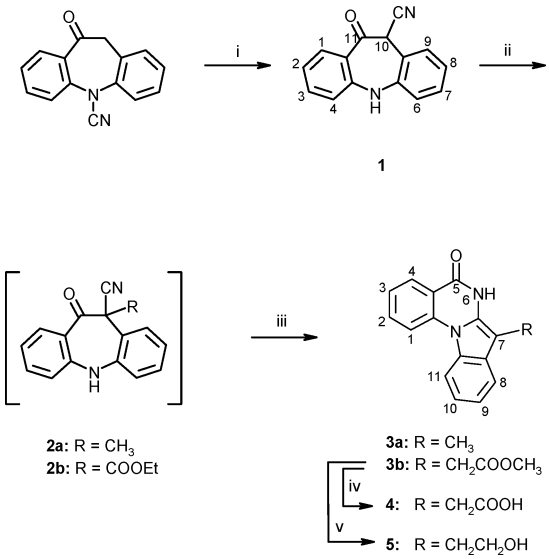

hydrolysis of the ester **3b**. The hydroxyethyl derivative **5** resulted from lithium borohydride reduction of **3b**.

Conclusion

We have identified a 7-substitued indoloquinazoline compound as a novel inhibitor of protein kinase CK2 by virtual screening of 400 000 compounds, of which a dozen were selected for actual testing in a biochemical assay. The compound inhibits the enzymatic activity of CK2 with an IC_{50} value of 80 nM, making it the most potent inhibitor of this enzyme ever reported. Its high potency, associated with high selectivity, provides a valuable tool for the study of the biological function of CK2.

The reported work clearly shows that large database docking in conjunction with appropriate scoring and filtering processes can be useful in medicinal chemistry. This approach has reached a maturation stage where it can start contributing to the lead finding process. At the time of this study, nearly one month was necessary to complete such a docking experiment in our laboratory settings. The Grid computing architecture recently developed by United Devices[29] allows us to now perform the same task in less than five working days using the power of hundreds of desktop PC's. High-throughput docking has therefore acquired the status of a routine screening technique.

Experimental Section

Homology Modeling. The sequence of human CK2α was obtained from SWISS-PROT[30] (entry P19138). The Fasta search option available in the Protein Data Bank[31] helped to identify several structural templates on which to base the homology model. The crystallographic structure of *Zea mays* CK2α[32] in complex with an ATP analogue (PDB code 1DAW

from the Protein Databank) was finally chosen as the template because of its high resolution (2.2 Å) and the high sequence similarity existing between the human and *Zea mays* enzymes (92% sequence similarity). The sequences were aligned in the homology module of Insight II[33] using the default parameters (scoring matrix: mutation, gap penalty: 6, and gap length penalty: 1.65). On the basis of the resulting alignment, shown in Figure 1, the 3D structure of human CK2α was modeled using the WhatIf[34] program with the default parameters (PIRPSQ module, BLDPIR command). Hydrogen atoms and Kollman united atom charges were subsequently added using the biopolymer module of Sybyl.[35] The model thus obtained was used without further energy refinement.

Structure-Based Database Search. For the docking experiment, a subset of around 400 000 chemical entities were selected from our corporate compound collection. This subset was created using filters to eliminate molecules that have unwanted atoms or fragments (e.g., P, Si) and to avoid molecules with a molecular weight inferior to 25 or superior to 1000. Starting from the two-dimensional structures, the 3D coordinates of all compounds were generated using Corina.[36] Hydrogen atoms, protonation states and Gasteiger−Marsili[37] atomic charges were then added using a Sybyl SPL macro, and the final coordinates were stored in a multimol2 file.

Compounds were flexibly docked using the DOCK 4.01 docking software package.[38] In the DOCK method the binding site is represented geometrically as a set of overlapping spheres[39] (docking spheres) which are created using the computer program Sphgen.[38] Although a large number of spheres may represent the 3D structure of the binding site more accurately, in practice one has to limit the number of spheres for computational efficiency. Restricting the covered area to the part of the ATP binding site where kinase inhibitors are known to make crucial interactions, 15 spheres were finally retained. The docking protocol chosen in this work slightly differs from those usually reported in the literature where DOCK is used giving the standard values to the parameters. A detailed discussion on the use of DOCK 4 can be found in ref 39. The whole molecule approach (anchor_search option set to no) was used in combination with a manual matching (maximum_orientations set to 1000, nodes_minimum set to 4, and distance_tolerance set to 0.3 Å). All docking poses were energy minimized using 100 iterations and 10 minimization cycles. The poses were evaluated and the ligands ranked using the energy scoring function of DOCK which is an interaction force field score that includes van der Waals and electrostatic terms. The use of the energy scoring function in combination with a united atom model has proven to give better results in a systematic assessment conducted internally. This protocol leads to an average processing time of 42 s per compound and per CPU on a Silicon Graphics Origin 2000 computer possessing 8 R10000 processors. To avoid highly flexible, very small, or very large ligands, several filters were applied prior to docking. Compounds with more than 12 flexible bonds were thus discarded as well as compounds with less than 6 or more than 60 heavy atoms.

Compounds with a docking score inferior or equal to the value of −35 kcal/mol were retained in a first step. This arbitrary selection gave 12 428 compounds which were then filtered according two different criterions. In the first stage, only compounds presenting two hydrogen bond interactions with the backbone of the hinge segment, either at residue Val 116 alone or simultaneously at Val 116 and Glu 114, were retained. The binding modes of the compounds were then evaluated using the scoring function of Wang et al.[25] This empirical scoring fuction contains a supplementary term accounting for solvation/desolvation effects compared to the DOCK energy function. Compounds with a score inferior to 5 according to the Wang function were discarded. The remaining 1592 compounds docked in the ATP pocket of CK2 were visually inspected. After this inspection, 12 compounds were selected to be experimentally tested in the CK2 inhibition assay. These 12 compounds were judged particularly promising because they presented high structural complementarity with the ATP pocket. Unlike many other docked compounds, they did not show any electrostatic or hydrophobic mismatch with the binding site and had no apparent conformational strain. In addition, they possessed few entropically unfavorable rotatable bonds.

Chemical Synthesis And Starting Material. Melting points (uncorrected) were determined using a Büchi 510 apparatus. MS (mass spectra) were recorded with a Micromass Platform II using electron spray ionization (positive or negative mode). ^{1}H and ^{13}C nuclear magnetic resonance spectroscopy was performed on Brucker and Varian instruments at force fields of 200 to 500 MHz for ^{1}H NMR and 100 MHz for ^{13}C NMR. Peak assignment was performed using COSY, HSQC, and HMBC techniques. The starting material 10-oxo-10,11-dihydrodibenzo[*b*,*f*]azepine-5-carbonitrile (CAN: 78880-65-6, EINECS: 2789984) is available in bulk quantities and is used in the production synthesis of the antiepileptic drug Trileptal.[40]

11-Oxo-10,11-dihydro-5*H*-dibenzo[*b*,*f*]azepine-10-carbonitrile (1). Solid potassium *tert*-butylate (62.3 g, 544 mmol) was added in four portions to a solution of 10-oxo-10,11-dihydrodibenzo[*b*,*f*]azepine-5-carbonitrile (75 g, 320 mmol) in 2.5 L of 1,2-dichloroethane at rt within 2 h. Thereafter a mixture of acetic acid (32.2 mL) and 300 mL of ice-cold water was slowly added. The resulting suspension was stirred for 10 min, cyclohexane (650 mL) was added, and stirring continued for 1 h at 0 °C. The precipitate was collected by filtration, washed with water (300 mL), and cyclohexane (300 mL). The crude product was recrystallized from 2.5 L of boiling EtOH upon concentration to 1.2 L of solvent followed by slow cooling to yield 11-oxo-10,11-dihydro-5*H*-dibenzo[*b*,*f*]azepine-10-carbonitrile **1** (56.6 g, 75%) as pale-yellow crystals. mp: 195−197 °C; ^{1}H NMR (d_6-DMSO, 400 MHz) mixture of keto−enol tautomers, therefore no peak assignment possible: δ 5.40 (s, 0.60H), 6.95−7.06 (m, 2.23H), 7.12−7.18 (m, 0.81H), 7.30−7.45 (m, 3.38H), 7.51−7.59 (m, 1.69H), 7.80−7.85 (m(d), 0.65H), 9.84 (s, 0.65H); ^{13}C NMR (d_6-DMSO, 100 MHz) all signals double due to keto−enol tautomerism: δ 49.41, 91.29, 116.80, 119.32, 119.73, 119.97, 120.35, 120.68, 121.07, 121.25, 121.35, 121.79, 123.25, 124.30, 125.67, 125.88, 126.45, 127.20, 128.70, 129.12, 129.57, 129.99. 130.62, 133.54, 135.34, 141.49, 147.53, 150.00, 153.17, 181.62; MS (ES, neg.) *m*/*z* 233 (M − 1), MS (ES, pos.) *m*/*z* 235 (M + 1); HR-MS *m*/*z* 233.0713 [(M − H) calcd for $C_{15}H_{10}N_3O$ 233.0715]; Anal. ($C_{15}H_{10}N_2O$) C, H, N.

10-Methyl-11-oxo-10,11-dihydro-5*H*-dibenzo[*b*,*f*]azepine-10-carbonitrile (2a). To a cooled (5 °C) mixture of **1** (25 g, 106.7 mmol) and potassium carbonate (18 g, 130.2 mmol) in DMF (60 mL) under nitrogen was added methyl iodide (7.8 mL, 124.9 mmol)) within 10 min. The resulting orange suspension was stirred at 0 °C for 30 min then at rt for 2 h before toluene (6 mL) was added dropwise, followed by water (100 mL). Precipitation of the product was forced by cooling to 0 °C. 10-Methyl-11-oxo-10,11-dihydro-5*H*-dibenzo[*b*,*f*]azepine-10-carbonitrile **2a** (14.2 g, 54%) was obtained as crude yellow-orange crystals. mp: 174−175 °C; ^{1}H NMR (d_6-DMSO, 400 MHz) δ 1.91 (s, 3H, CH_3), 6.97 (t(dd), J_{2-1} = 8.03 Hz, J_{2-3} = 7.45 Hz, 1H, H-2), 7.27−7.31 (m, 1H, H-7), 7.43−7.44 (m, 3H, H-4, H-5, H-6), 7.52 (d, J_{8-7} = 7.94 Hz, 1H, H-8), 7.57 (ddd, J_{3-2} = 7.45 Hz, J_{3-4} = 7.95 Hz, J_{3-1} = 1.58 Hz, 1H, H-3), 7.75 (dd, J_{1-2} = 8.03 Hz, J_{1-3} = 1.58 Hz, 1H, H-1), 10.14 (s, 1H, H−N); ^{13}C NMR (d_6-DMSO, 100 MHz) δ 19.57 (CH_3), 119.61 (C-2), 119.96 (C-1a), 120.02 (C-4), 120.26 (C-10), 121.47 (C-9a), 121.88 (C-6), 125.42 (C-8), 126.81 (C-9), 130.34 (C-7), 131.30 (C-1), 135.17 (C-3 and CN), 140.76 (C-6a), 145.79 (C-4a), 183.40 (C-11); MS (ES, neg.) *m*/*z* 247 (M-1); HR-MS *m*/*z* 247.0872 [(M − H) calcd for $C_{16}H_{12}N_2O$ 247.0871]; Anal. ($C_{16}H_{12}N_2O$) C, H, N.

7-Methyl-6*H*-indolo[1,2-*a*]quinazolin-5-one (3a). Sodium methoxide solution (20.3 mL, 112.77 mmol, 30% solution in MeOH) was added to **2a** (10 g, 40.28 mmol) in MeOH (220 mL) at rt, then immediately heated to 65 °C for 3 h. After stirring at rt overnight, the yellow residue was heated at 60 °C, and a mixture of acetic acid (10 mL) in water (220 mL) was added dropwise. The resulting suspension was stirred at

0 °C for 1 h and the 7-methyl-6*H*-indolo[1,2-*a*]quinazolin-5-one (**3a**) collected by filtration (8.8 g, 88%) as yellow crystals. mp: 298−300 °C, decomp; ^{1}H NMR (d_6-DMSO, 400 MHz) δ 2.27 (s, 3H, CH_3), 7.22 (dd, J_{10-11} = 8.28 Hz, J_{10-9} = 7.11 Hz, 1H, H-10), 7.26 (dd, J_{9-10} = 7.11 Hz, J_{9-8} = 7.53 Hz, 1H, H-9), 7.37 (dd, J_{3-2} = 7.70 Hz, J_{3-4} = 7.78 Hz, 1H, H-3), 7.51 (d, J_{8-9} = 7.53 Hz, 1H, H-8), 7.84 (ddd, J_{2-3} = 7.70 Hz, J_{2-1} = 8.45 Hz, J_{2-4} = 1.42 Hz, 1H, H-2), 8.18 (dd, J_{4-3} = 7.78 Hz, J_{4-2} = 1.42 Hz, 1H, H-4), 8.25 (d, J_{11-10} = 8.28 Hz, 1H, H-11), 8.41 (d, J_{1-2} = 8.45 Hz, 1H, H-1), 11.79 (s br, 1H, H−N); ^{13}C NMR (d_6-DMSO, 100 MHz) δ 7.53 (CH_3), 90.34 (C-7), 113.78 (C-11), 115.71 (C-1), 117.29 (C-4a), 118.19 (C-8), 121.46 (C-10), 122.68 (C-9), 123.96 (C-3), 129.59 (C-4), 130.43 (C-11a), 131.54 (C-7a), 133.50 (C-6a), 135.83 (C-2), 139.86 (C-1a), 159.64 (C-5); MS (ES, neg.) *m*/*z* 247 (M − 1), MS (ES, pos.) *m*/*z* 249 (M + 1); HR-MS *m*/*z* 249.1028 [(M + H) calcd for $C_{16}H_{12}N_2O$ 249.1028; Anal. ($C_{16}H_{12}N_2O$) C, H, N.

(10-Cyano-11-oxo-10,11-dihydro-5*H*-dibenzo[*b*,*f*]azepin-10-yl)acetic Acid Ethyl Ester (2b). The ethyl acetate derivative **2b** was synthesized in analogy to **2a** from **1** and ethyl bromoacetate. The resulting crude orange oil was directly used for the following conversion into **3b**. MS (ES, pos.) *m*/*z* 321 (M + 1).

(5-Oxo-5,6-dihydroindolo[1,2-*a*]quinazolin-7-yl)acetic Acid Methyl Ester (3b). The methyl ester **3b** was synthesized from **2b** (14.7 g, 45.89 mmol) in analogy to the procedure used for **3a**. Transesterification occurred from ethyl to methyl ester. (5-Oxo-5,6-dihydroindolo[1,2-*a*]quinazolin-7-yl)acetic acid methyl ester (**3b**) (9.4 g, 67%) was obtained as yellow crystals. mp: 245−252 °C, decomp; ^{1}H NMR (d_6-DMSO, 500 MHz) δ 3.62 (s, 3H, OCH_3), 3.94 (s, 2H, CH_2), 7.22−7.27 (m, 2H, H9 and H-10), 7.41 (dd, J_{3-2} = 7.4 Hz, J_{3-4} = 7.61 Hz, 1H, H-3), 7.48−7.50 (m, 1H, H-8), 7.87 (ddd, J_{2-1} = 8.44 Hz, J_{2-3} = 7.53 Hz, J_{2-4} = 1.30 Hz, 1H, H-2), 8.20 (dd, J_{4-3} = 7.70 Hz, J_{4-2} = 1.26 Hz, 1H, H-4), 8.25 (m, 1H, H-11), 8.45 (d, J_{1-2} = 8.45 Hz, 1H, H-1), 11.93 (s, 1H, H−N); ^{13}C NMR (d_6-DMSO, 125 MHz) δ 27.27 (CH_2), 51.74 (OCH_3), 87.77 (C-7), 113.16 (C-11), 115.18 (C-1), 116.34 (C-4a), 117.55 (C-8), 120.99 (C-10), 122.16 (C-9), 123.60 (C-3), 128.76 (C-4), 129.60 and 129.89 (C-7a and C-11a), 133.50 (C-6a), 135.30 (C-2), 138.76 (C-1a), 158.57 (CONH), 171.51 (COO); MS (ES, neg.) *m*/*z* 305 (M − 1), MS (ES, pos.) *m*/*z* 307 (M + 1); HR-MS *m*/*z* 307.1085 [(M + H) calcd for $C_{18}H_{14}N_2O_3$ 307.1083; Anal. ($C_{18}H_{14}N_2O_3$) C, H, N.

(5-Oxo-5,6-dihydroindolo[1,2-*a*]quinazolin-7-yl)acetic Acid (4). A slurry of **3b** (5.0 g, 16.32 mmol) in DMSO (50 mL) was treated with 1 N aqueous sodium hydroxyde solution (45.7 mL, 45.7 mmol) at rt. A clear solution was observed followed by precipitation of a yellow solid. The mixture was diluted with water (150 mL) and cooled to 5 °C, and acetic acid (20 mL) was added. After 45 min, (5-oxo-5,6-dihydroindolo[1,2-*a*]quinazolin-7-yl)acetic acid **4** was obtained by filtration as yellow crystals (4.54 g, 95%). mp: 234−236 °C, decomp.; ^{1}H NMR (d_6-DMSO, 500 MHz) δ 3.85 (s, 2H, CH_2), 7.22−7.30 (m, 2H, H-9 and H-10), 7.42 (dd, J_{3-2} = 7.39 Hz, J_{3-4} = 7.79 Hz, 1H, H-3), 7.49−7.55 (m, 1H, H-8), 7.88 (ddd, J_{2-1} = 8.46 Hz, J_{2-3} = 7.39 Hz, J_{2-4} = 1.75 Hz, 1H, H-2), 8.20 (dd, J_{4-3} = 7.79 Hz, J_{4-2} = 1.61 Hz, 1H, H-4), 8.29 (dd, J_{11-10} = 8.46 Hz, J_{11-9} = 2.15 Hz, 1H, H-11), 8.47 (d, J_{1-2} = 8.46 Hz, 1H, H-1), 11.92 (s br, 1H, COOH), 12.28 (s br, 1H, NH); ^{13}C NMR (d_6-DMSO, 125 MHz) δ 27.64 (CH_2), 87.59 (C-7), 113.13 (C-11), 115.15 (C-1), 116.34 (C-4a), 117.59 (C-8), 120.91 (C-10), 122.10 (C-9), 123.54 (C-3), 128.77 (C-4), 129.60 (C-11a), 130.05 (C-7a), 133.35 (C-6a), 135.30 (C-2), 138.82 (C-1a), 158.57 (CONH), 172.60 (COOH); MS (ES, neg.) *m*/*z* 291 (M − 1), MS (ES, pos.) *m*/*z* 293 (M + 1); HR-MS *m*/*z* 293.0928 [(M + H) calcd for $C_{17}H_{12}N_2O_3$ 293.0926; Anal. ($C_{17}H_{12}N_2O_3$) C, H, N.

7-(2-Hydroxyethyl)-6*H*-indolo[1,2-*a*]quinazolin-5-one (5). A THF solution (25 mL) of lithium borohydride (0.62 g, 28.56 mmol) was added dropwise to a suspension of **3b** (2.5 g, 8.16 mmol) in THF (40 mL) at rt. After the exothermic reaction had ceased the mixture was heated at 75 °C for 18 h. At 10 °C, ethanol (100 mL) and water (20 mL) were added, further chilled to 0 °C, and acidified to pH = 7 with 2 N hydrochloric acid. The yellow crystalline 7-(2-hydroxyethyl)-6*H*-indolo[1,2-*a*]quinazolin-5-one (**5**) (1.6 g, 71%) was collected by filtration, washed with water and ethanol, and dried in vacuo at 60 °C. mp: 240−249 °C, decomp.; ^{1}H NMR (d_6-DMSO, 500 MHz) δ 2.96 (t, *J* = 6.58 Hz, 2H, CH_2CH_2OH), 3.61 (t, *J* = 6.59 Hz, 2H, CH_2OH), 4.63−4.87 (br, 1H, OH), 7.21−7.27 (m, 2H, H-9 and H-10), 7.38 (dd, J_{3-2} = 7.79 Hz, J_{3-4} = 7.79 Hz, 1H, H-3), 7.58 (dd, J_{8-9} = 7.12, J_{8-10} = 1.61, Hz, 1H, H-8), 7.85 (ddd, J_{2-3} = 7.79 Hz, J_{2-1} = 8.46 Hz, J_{2-4} = 1.61 Hz, 1H, H-2), 8.17 (dd, J_{4-3} = 7.79 Hz, J_{4-2} = 1.48 Hz, 1H, H-4), 8.26 (d, J_{11-10} = 7.65 Hz, 1H, H-11), 8.41 (d, J_{1-2} = 8.47 Hz, 1H, H-1), 11.66−11.82 (s br, 1H, H−N); ^{13}C NMR (d_6-DMSO, 125 MHz) δ 25.34 (CH_2), 60.85 (CH_2OH), 92.40 (C-7), 113.07 (C-11), 115.09 (C-1), 116.38 (C-4a), 117.73 (C-8), 120.70 (C-10), 121.91 (C-9), 123.30 (C-3), 128.76 (C-4), 129.67 (C-11a), 130.33 (C-7a), 132.67 (C-6a), 135.19 (C-2), 138.95 (C-1a), 158.50 (CONH); MS (ES, neg.) *m*/*z* 277 (M-1), MS (ES, pos.) *m*/*z* 279 (M + 1); HRMS *m*/*z* 277.0974 [(M−H) calcd for $C_{17}H_{14}N_2O_2$ 279.0977; Anal. ($C_{17}H_{14}N_2O_2$) C, H, N.

Kinase Inhibition Assays. The CK2 inhibition assay used is described in ref 41. Briefly, one looks at the ability of a compound to inhibit the phosphorylation of a peptide substrate (RRRADDSDDDDD) by native CK2 purified from rat liver. Human (SWISS-PROT entry P19138) and rat CK2α (SWISS-PROT entry P19139) have 100% sequence identity. Therefore, similar compound potencies as in the rat enzyme assay would be expected in a human enzyme assay. This has been checked for some inhibitors[11] and has proven to be the case. The selectivity kinase inhibition assays reported in Table 2 were performed under conditions optimized for each kinase and with ATP concentrations similar to the K_m of the respective enzyme toward ATP: 8.0 μM (KDR, Flt-1, FGFR-1, Tek), 1.0 μM (PDGFR-β, c-Kit, c-Met), 13 μM (Flt-4), 5 μM (c-abl), 2.0 μM (Her-1, Her-2), 20 μM (c-Src), 30 μM (IGF-1R), 7.5 μM (CDK1), and 50 μM (PKA). For tyrosine kinases, filter binding assays using recombinant GST-fused kinase domains of the receptors expressed in baculovirus and purified over glutathione sepharose were employed. [^{33} P]-ATP was used as the phosphate donor, and the polyGluTyr (4:1) peptide was used as the acceptor. The CDK1 and PKA assays are described in refs 42 and 43, respectively.

Acknowledgment. The authors wish to acknowledge Corinne Marx and Simon Pfister for technical support.

References

(1) Pinna, L. A. Protein kinase CK2: a challenge to canons. *J. Cell Sci*. **2002**, *115*, 3873−3878.
(2) Litchfield, D. W. Protein kinase CK2: structure, regulation and role in cellular decisions of life and death. *Biochem. J*. **2003**, *369*, 1−15.
(3) Ahmed, K.; Gerber, D. A.; Cochet, C. Joining the cell survival squad: an emerging role for protein kinase CK2. *Trends Cell Biol*. **2002**, *12*, 226−230.
(4) Tawfic, S.; Yu, S.; Wang, H.; Faust, R.; Davis, A.; Ahmed, K. Protein kinase CK2 signal in neoplasia. *Histol. Histopathol*. **2001**, *16*, 573−582.
(5) Guerra, B.; Issinger, O. G. Protein kinase CK2 and its role in cellular proliferation, development and pathology. *Electrophoresis* **1999**, *20*, 391−408.
(6) Seldin, D. C.; Leder, P. Casein kinase 2α-induced murine lymphoma: relation to Teilleriosis in cattle. *Science*. **1995**, *267*, 894−897.
(7) Sarno, S.; Moro, S.; Meggio, F.; Zagotto, G.; Dal Ben, D.; Ghisellini, P.; Battistutta, R.; Zanotti, G.; Pinna, L. A. Toward the rational design of protein kinase casein kinase-2 inhibitors. *Pharmacol. Ther*. **2002**, *93*, 159−168.
(8) Battistutta, R.; De Moliner, E.; Sarno, S.; Zanotti, G.; Pinna, L. A. Structural features underlying selective inhibition of protein kinase CK2 by ATP site-directed tetrabromo-2-benzotriazole. *Protein Sci*. **2001**, *10*, 2200−2206.
(9) Battistutta, R.; Sarno, S.; De Moliner, E.; Papinutto, E.; Zanotti, G.; Pinna, L. A. The replacement of ATP by the competitive inhibitor emodin induces conformational modifications in the catalytic site of protein kinase CK2. *J. Biol. Chem*. **2000**, *275*, 29618−29622.

(10) De Moliner, E.; Moro, S.; Sarno, S.; Zagotto, G.; Zanotti, G.; Pinna, L. A.; Battistutta, R. Inhibition of protein kinase CK2 by anthraquinone-related compounds. A structural insight. *J. Biol. Chem*. **2003**, *278*, 1831−1836.
(11) Sarno, S.; Reddy, H.; Meggio, F.; Ruzzene, M.; Davies, S. P.; Donella-Deana, A.; Shugar, D.; Pinna, L. A. Selectivity of 4,5,6,7-tetrabromobenzotriazole, an ATP site-directed inhibitor of protein kinase CK2 ('casein kinase-2'). *FEBS Lett.* **2001**, *496*, 44−48.
(12) Ruzzene, M.; Penzo, D.; Pinna, L. A. Protein kinase CK2 inhibitor 4,5,6,7-tetrabromobenzotriazole (TBB) induces apoptosis and caspase-dependent degradation of haematopoietic lineage cell-specific protein 1 (HS1) in Jurkat cells. *Biochem. J*. **2002**, *364*, 41−47.
(13) Shoichet, B. K.; McGovern, S. L.; Wei, B.; Irwin, J. J. Lead discovery using molecular docking. *Curr. Opin. Chem. Biol.* **2002**, *6*, 439−446.
(14) Schneider, G.; Böhm, H.-J. Virtual screening and fast automated docking methods. *Drug Discov. Today* **2002**, *7*, 64−70.
(15) Niefind, K.; Guerra, B.; Ermakowa, I.; Issinger, O. G. Crystal structure of human protein kinase CK2: insights into basic properties of the CK2 holoenzyme. *EMBO J*. **2001**, *20*, 5320−5331.
(16) Kuntz, I. D.; Meng, E. C.; Shoichet, B. K. Structure-based molecular design [Review]. *Acc. Chem. Res.* **1994**, *27*, 117−123.
(17) Filikov, A. V.; James, T. L. Structure-based design of ligands for protein basic domains: application to the HIV-1 Tat protein. *J. Comput.-Aided Mol. Des.* **1998**, *12*, 229−240.
(18) Shoichet, B. K.; Stroud, R. M.; Santi, D. V.; Kuntz, I. D.; Perry, K. M. Structure-based discovery of inhibitors of thymidylate synthase. *Science* **1993**, *259*, 1445−1450.
(19) Bodian, D. L.; Yamasaki, R. B.; Buswell, R. L.; Stearns, J. F.; White, J. M.; Kuntz, I. D. Inhibition of the fusion-inducing conformational change of influenza hemagglutinin by benzoquinones and hydroquinones. *Biochemistry* **1993**, *32*, 2967−2978.
(20) Ring, C. S.; Sun, E.; McKerrow, J. H.; Lee, G. K.; Rosenthal, P. J.; Kuntz, I. D.; Cohen, F. E. Structure-based inhibitor design by using protein models for the development of antiparasitic agents. *Proc. Natl. Acad. Sci.* **1993**, *90*, 3583−3587.
(21) Boehm, H.-J.; Stahl, M. The use of scoring functions in drug discovery applications. In *Reviews in Computational Chemistry*; Lipkowitz K. B., Boyd, D. B., Eds.; Wiley-VCH: New York, 2002; Vol. 18, pp 41−87.
(22) Toledo, L. M.; Lydon, N. B.; Elbaum, D. The Structure-based design of ATP-site directed protein kinase inhibitors. *Curr. Med. Chem*. **1999**, *6*, 775−805.
(23) Traxler, P.; Furet, P. Strategies toward the design of novel and selective protein tyrosine kinase inhibitors. *Pharmacol. Ther.* **1999**, *82*, 195−206.
(24) Furet, P.; Meyer, T.; Strauss, A.; Raccuglia, S.; Rondeau, J. M. Structure-based design and protein X-ray analysis of a protein kinase inhibitor. *Bioorg. Med. Chem. Lett*. **2002**, *12*, 221−224.
(25) Wang, R.; Liu, L.; Lai, L.; Tang, Y. SCORE: A New Empirical Method for Structure-Based Estimation of Binding Affinities. *J. Mol. Model.* **1998**, *4*, 379−394.
(26) Moore, J. A.; Sutherland, G. J.; Sowerby, R.; Kelly, E. G.; Palermo, S.; Webster, W. Reactions of anthranilamide and *o*-aminoacetophenone with benzil and benzoin. *J. Org. Chem*. **1969**, *34*, 887−892.
(27) Moehrle, H.; Seidel, Ch. M. Quinolinones as starting products for pentacyclic heterocycles. *Arch. Pharm. (Weinheim, Ger.)* **1974**, *307*, 785−791.
(28) described in lit.: Zimmermann, K.; Portmann, R.; Rigel, D. F. Preparation of indoloquinazolinones as PARP inhibitors. PCT Int. Appl. WO 0206284 A1, 2001**.**
(29) United Devices, Austin, TX (see website: http://www.ud.com).
(30) Bairoch, A.; Boeckmann, B. The SWISS-PROT protein sequence data bank: current status. *Nucleic Acids Res*. **1994**, *22*, 3578−3580.
(31) Bernstein, F. C.; Koetzle, T. F.; Williams, G. J. B.; Meyer, E. F.; Brice, M. D.; Rodgers, J. R.; Kennard, O.; Shimanouchi, T.; Tasumi, M. The Protein Data Bank: a Computer-based Archival File for Macromolecular Structures. *J. Mol. Biol.* **1977**, *112*, 535−542.
(32) Niefind, K.; Putter, M.; Guerra, B.; Issinger, O. G.; Schomburg, D. GTP plus water mimic ATP in the active site of protein kinase CK2. *Nat. Struct. Biol.* **1999**, *12*, 1100−1103.
(33) Insight II, Accelrys, San Diego, CA.
(34) Vriend, G.; WHAT IF: A molecular modeling and drug design program. *J. Mol. Graph*. **1990**, *8*, 52−56.
(35) Tripos Inc. Sybyl 6.6. St. Louis MO, 2001.
(36) Gasteiger, J.; Rudolph, C.; Sadowski, J. Automatic generation of 3D atomic coordinates for organic molecules. *Tetrahedron Comput. Methodol*. **1990**, *3*, 537−547.
(37) Gasteiger, J.; Marsili, M. Iterative Partial Equalization of Orbital Electronegativity − A Rapid Access to Atomic Charges. *Tetrahedron* **1980**, *36*, 3219−3228.
(38) Kuntz, I. D.; Blaney, J. M.; Oatley, S. J.; Langridge, R. T.; Ferrin, T. E. A geometric approach to macromolecule-ligand interactions. *J. Mol. Biol*. **1982**, *161*, 269−288.
(39) Ewing, T. J. A.; Kuntz, I. D. Critical evaluation of search algorithms for automated molecular docking and database screening. *J. Comput. Chem*. **1997**, *18*, 1175−1189.
(40) described in lit.: Citterio, A.; Breviglieri, G.; Bruno, G. Eur. Pat. Appl. (2001), EP 1127877. A2 and Aufderhaar, E. Eur. Pat. Appl. EP 28028, 1981.
(41) Meggio, F.; Donella Deana, A.; Ruzzene, M.; Brunati, A. M.; Cesaro, L.; Guerra, B.; Meyer, T.; Mett, H.; Fabbro, D.; Furet, P.; Dobrowolska, G.; Pinna, L. A. Different susceptibility of protein kinases to staurosporine inhibition. Kinetic studies and molecular bases for the resistance of protein kinase CK2. *Eur. J. Biochem*. **1995**, *234*, 317−322.
(42) Rialet, V.; Meijer, L. A New Screening Test for Antimitotic compounds affinity-immobilized on p13suc1 -coated microtitration plates. *Anticancer Res*. **1991**, *11*, 1581−1590.
(43) Meyer, T.; Regenass, U.; Fabbro, D.; Alteri, E.; Roesel, J.; Muller, M.; Caravatti, G.; Matter, A. A derivative of staurosporine (CGP 41 251) shows selectivity for protein kinase C inhibition and in vitro anti-proliferative as well as in vivo antitumor activity. *Int. J. Cancer* **1989**, *43*, 851−856.

JM030827E